Science Advances
AAAS

advances.sciencemag.org/cgi/content/full/6/22/eaba4243/DC1

Supplementary Materials for

Reconstructing the time since death using noninvasive thermometry and numerical analysis

Leah S. Wilk, Richelle J. M. Hoveling, Gerda J. Edelman, Huub J. J. Hardy, Sebastiaan van Schouwen, Harry van Venrooij, Maurice C. G. Aalders*

*Corresponding author. Email: m.c.aalders@amsterdamumc.nl

Published 29 May 2020, *Sci. Adv.* **6**, eaba4243 (2020)
DOI: 10.1126/sciadv.aba4243

This PDF file includes:

Supplementary Materials

Section S1. Theory

Post-mortem temperature change of the human body

With its death, the human body ceases to thermoregulate and given a temperature gradient between the body and its surroundings, heat will be exchanged until a state of thermal equilibrium is reached. This exchange of heat will become apparent as a change in body temperature. The dynamics of this process are fully determined by the magnitude of the thermal gradient and the specific thermal properties of the involved materials. Consequently, knowledge of these thermal properties and timely (prior to thermal equilibrium) probing of this process should allow the reconstruction of the PMI.

The dissipation of heat and the associated change in temperature in its most general form are described by the transient heat equation. As such, an analytical solution describing this process for the complex case of a human body does not exist. Alternatively, this heat transport can be modelled as a steady-state combination of three distinct heat transfer processes: conduction, convection and radiation. This, in turn, allows numerical simulation of the body temperature evolution using finite difference methods. Here, the spatio-temporal domain of the heat exchange process is divided into intervals and derivatives are approximated by finite differences between neighboring elements.

Heat exchange phenomena

The heat transfer phenomena of the composite model and their dependence on physical properties can be stated as follows (*37*):

(i) Conduction: $\Delta E = h_{cond} A \Delta T \Delta t$ where $h_{cond} = \frac{\lambda}{l}$

(ii) Convection: $\Delta E = h_{conv} A \Delta T \Delta t$ where $h_{conv} = \frac{Nu\,\lambda}{L}$

(iii) Radiation: $\Delta E = h_{rad} A \Delta T \Delta t$ where $h_{rad} = \sigma \epsilon (T_b^2 + T_\infty^2)(T_b + T_\infty)$

Expression (i) follows directly from Fourier's law of heat transfer. We use this expression to calculate the heat transfer between the body and solid materials, such as clothes and the substrate on which the body is positioned. In order to include convective heat transport (*e.g.* through air or water), relation (i) is modified to equation (ii) using the fluid mechanical description of gases. Finally, (iii) is a direct consequence of the Stefan-Boltzmann equation for radiative energy transfer under the assumption that the difference between T_b and T_∞ is small. Here, ΔE denotes the amount of heat energy [J] transported through the area A [m^2] in the time interval Δt [s], driven and regulated by the finite difference in temperature ΔT [K] and the conductance $h_{cond/conv/rad}$ [$Wm^{-2}K^{-1}$], respectively. Furthermore, the quantities λ, l, L, Nu, σ, ϵ, T_b, T_∞, denote thermal conductivity [$Wm^{-1}K^{-1}$], length [m], the characteristic length for convective heat transfer (*33*) [m], the dimensionless Nusselt number for combined free and forced convection (*33, 38*), the Stefan-Boltzmann constant [$Wm^{-2}K^{-4}$], the dimensionless emissivity, as well as the temperatures of the body and the environment [K], respectively. The Nusselt number for combined free and forced convection is computed as follows: $({Nu_{free}}^3 + {Nu_{forced}}^3)^{\frac{1}{3}}$. The Nusselt number for free convection is given by: $Nu_{free} = 0.63Gr^{0.25}Pr^{0.25}$ (*38*), where Gr and Pr denote the Grasshof number for a vertical flat plate and the Prandtl number, respectively. Nu_{forced} depends on the Reynolds number, *i.e.* the flow regime, of the surrounding fluid (*33*). In the laminar flow regime, we compute Nu_{forced} by averaging the Nusselt numbers for flow along a plane and a cylinder (as an approximation of the human body):

$$Nu = \left(0.3 + \frac{0.62 Re^{0.5} Pr^{\frac{1}{3}}}{\left(1 + \left(\frac{0.4}{Pr}\right)^{\frac{2}{3}}\right)^{0.25}} \cdot \left(1 + \left(\frac{Re}{2.82 \cdot 10^5}\right)^{0.625}\right)^{0.8} + \frac{0.6774 Re^{0.5} Pr^{\frac{1}{3}}}{\left(1 + \left(\frac{0.0468}{Pr}\right)^{\frac{2}{3}}\right)^{0.25}} \right)$$

In the turbulent regime, we calculate Nu_{forced} using:

$$Nu = \frac{0.6774 {Re_{crit}}^{0.5} Pr^{\frac{1}{3}}}{\left(1 + \left(\frac{0.0468}{Pr}\right)^{\frac{2}{3}}\right)^{0.25}} + 0.037\, Pr^{\frac{1}{3}} \left(Re^{0.8} - {Re_{crit}}^{0.8}\right)$$

Where Re and Re_{crit} denote the Reynolds and the critical Reynolds (in our case $Re_{crit} = 5*10^5$) number, respectively. To arrive at a comprehensive description of the local heat exchange, the conductances (h_{cond}, h_{conv} and h_{rad}) of (i)–(iii), also known as heat transfer coefficients, need to be combined appropriately. As conductance is additive in layered geometries such as the body, the total conductance is related to the individual conductances by the following expression (*39*):

(iv) $$\frac{1}{h_{total}} = \frac{1}{\sum_i h_i}$$

The change in temperature induced by the transferred heat is given by the following relation (*37*):

(v) $$dT = \frac{dE}{C} = \frac{dE}{mc} \approx \frac{\Delta E}{mc}$$

Here *C*, *c* and *m* denote heat capacity [JK^{-1}], specific heat capacity [$JK^{-1}kg^{-1}$] and mass [kg], respectively. Finally, combining (i) – (v) yields the desired estimate of the change in temperature as a function of time.

(vi) $$dT = \frac{h_{total}\, A\, \Delta t\, \Delta T}{mc}$$

Domain discretization

For the finite difference scheme an isotropic three-dimensional (cubic) mesh was used where the grid size Δx was set to 0.01m. This discretization yields the parameters A, ΔT and h_{total}, required to compute dT, denoting the contact surface, the temperature difference and the combined conductance for two neighboring cubes, respectively. Similarly, to obtain spatially-resolved temperature data for *different time points*, it is necessary to discretize the

time prior to equilibrium into finite time intervals Δt, which yields the last parameter needed to solve (vi).

Computational implementation

Simulation of the temperature evolution can be implemented as follows (*40*): first, a period is chosen for which the heat exchange is simulated, for example 24h. This period is then discretized into i finite time intervals of length Δt, *e.g.* 60s, yielding the number of computational iterations needed to simulate the temperature evolution in the chosen period, in this case $i = 1,2,3,\ldots1440$. Following this, the cubic mesh is generated automatically using the body dimensions provided by the user. The size of this mesh (number of grid points) varies with body size in order to optimize memory usage (in our case the largest number of grid points was 544320). Next, every cube in the grid is assigned a material, *i.e.* thermal properties, corresponding to either non-adipose tissue, adipose tissue, surrounding medium (*e.g.* air/water/solid substrate) or, if applicable, clothes. Subsequently, every cube is assigned an initial temperature, *e.g.* 37°C for the body or 4°C for the surrounding medium. These temperatures are then continuously updated for every time point ($t_i = i*\Delta t$) by computing (vi), where ΔT then refers to the temperature difference between neighboring cubes from the previous time step t_{i-1}. Here, we used an explicit scheme with Δt set to 60s and Δx set to 0.01m. This choice yields a numerically stable implementation as the largest thermal diffusivity assigned in any of our simulations was $0.26*10^{-6}$ m^2s^{-1}. Note, that only temperatures of body cubes (*i.e.* non-adipose / adipose tissue or clothes) are updated, as energy transferred to the surrounding media is assumed to dissipate and is hence excluded from any future heat exchange. Storing these updated temperatures for all body cubes for all t_i yields a spatially-resolved simulation of the temperature evolution (see Figure 5B) and consequently allows comparison with temperatures measured at specific body locations (see Figure 2). This, in turn, enables numeric reconstruction of the PMI by simulating the heat

exchange until a certain (location-specific) measured temperature is reached; the required number of time steps t_i then corresponds to the reconstructed PMI.

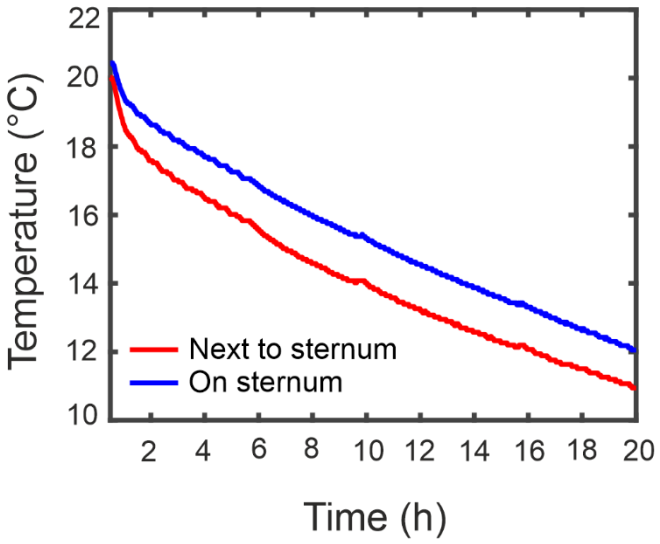

Fig. S1. Effect of sternum on chest temperature. Temperatures measured at different locations on the chest of a cooling deceased human body.

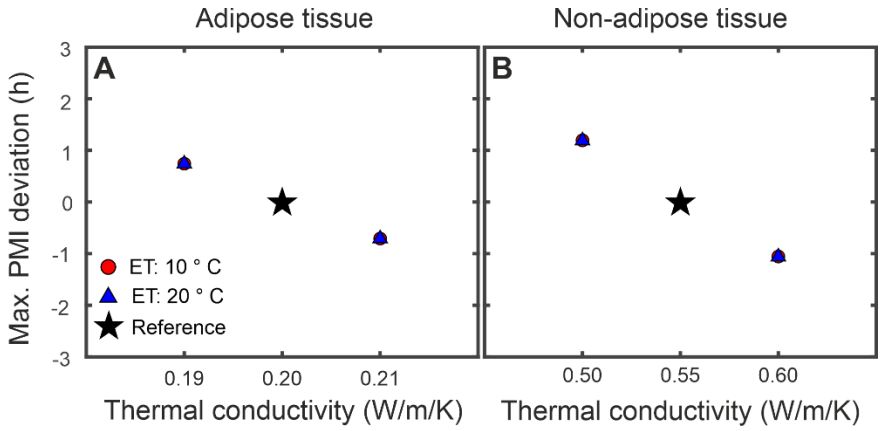

Fig. S2. Extended parameter sensitivity analysis. Effect of variation in the model input parameters (**A**) thermal conductivity of adipose tissue and (**B**) thermal conductivity of non-adipose tissue on the reconstructed PMIs. Circles and upward pointing triangles denote results for the parameter variations at 10° C and 20° C, respectively. Negative values of the PMI deviation correspond to an underestimation of the real PMI while positive values indicate overestimation.

Set #	Initial Body Temperature [°C]	Thermal Conductivity Clothes [$Wm^{-1}K^{-1}$]	Body Fat Percentage [%]
1 (Reference)	37	0.03	29
2	36	0.03	29
3	36.5	0.03	29
4	37.5	0.03	29
5	38	0.03	29
6	37	0.02	29
7	37	0.025	29
8	37	0.035	29
9	37	0.04	29
10	37	0.03	25
11	37	0.03	27
12	37	0.03	31
13	37	0.03	33

Table S1. Parameter sensitivity analysis. Parameter sets used for sensitivity analysis.

REFERENCES AND NOTES

1. F. A. Jaffe, *A Guide to Pathological Evidence for Lawyers and Police Officers* (Carswell, ed. 2, 1983).

2. J. Hayman, M. Oxenham, Biochemical methods of estimating the time since death. *Hum. Body Decompos.* **2016**, 53–90 (2016).

3. Y.-H. Lv, J.-L. Ma, H. Pan, H. Zhang, W.-C. Li, A.-M. Xue, H.-J. Wang, K.-J. Ma, L. Chen, RNA degradation as described by a mathematical model for postmortem interval determination. *J. Forensic Leg. Med.* **44**, 43–52 (2016).

4. W. Sturner, The vitreous humour: Postmortem potassium changes. *Lancet* **281**, 807–808 (1963).

5. Y. Ding, X. Li, Y. Guo, W. Duan, J. Ling, L. Zha, J. Yan, Y. Zou, J. Cai, Estimation of postmortem interval by vitreous potassium evaluation with a novel fluorescence aptasensor. *Sci. Rep.* **7**, 1868 (2017).

6. Z. M. Burcham, J. A. Hood, J. L. Pechal, K. L. Krausz, J. L. Bose, C. J. Schmidt, M. E. Benbow, H. R. Jordan, Fluorescently labeled bacteria provide insight on post-mortem microbial transmigration. *Forensic Sci. Int.* **264**, 63–69 (2016).

7. E. Locci, M. Stocchero, A. Noto, A. Chighine, L. Natali, P. E. Napoli, R. Caria, F. De-Giorgio, M. Nioi, E. d'Aloja, A ^{1}H NMR metabolomic approach for the estimation of the time since death using aqueous humour: An animal model. *Metabolomics* **15**, 76 (2019).

8. E. S. Estracanholli, C. Kurachi, J. R. Vicente, P. F. C. de Menezes, O. Castro e Silva Júnior, V. S. Bagnato, Determination of post-mortem interval using in situ tissue optical fluorescence. *Opt. Express*. **17**, 8185–8192 (2009).

9. J. R. Bendall, *The Structure and Function of Muscle* (Academic Press, 1973), pp. 243–309.

10. C. J. Polson, D. J. Gee, B. Knight, *The Essentials of Forensic Medicine* (Pergamon Press, 1985).

11. K. Reddy, E. J. Lowenstein, Forensics in dermatology: Part I. *J. Am. Acad. Dermatol.* **64**, 801–808 (2011).

12. S. Jaafara, L. D. M. Nokes, Examination of the eye as a means to determine the early postmortem period: A review of the literature. *Forensic Sci. Int.* **64**, 185–189 (1994).

13. L. D. Nokes, T. Flint, J. H. Williams, B. H. Knight, The application of eight reported temperature-based algorithms to calculate the postmortem interval. *Forensic Sci. Int.* **54**, 109–125 (1992).

14. T. K. Marshall, The use of body temperature in estimating the time of death and its limitations. *Med. Sci. Law* **9**, 178–182 (1969).

15. B. Knight, The evolution of methods for estimating the time of death from body temperature. *Forensic Sci. Int.* **36**, 47–55 (1988).

16. M. Hubig, H. Muggenthaler, S. Schenkl, G. Mall, Temperature-based death time estimation in near equilibrium: Asymptotic confidence interval estimation. *Forensic Sci. Int.* **290**, 189–195 (2018).

17. C. Henssge, B. Madea, Estimation of the time since death. *Forensic Sci. Int.* **165**, 182–184 (2007).

18. C. Henssge, Death time estimation in case work. I. The rectal temperature time of death nomogram. *Forensic Sci. Int.* **38**, 209–236 (1988).

19. L. Althaus, C. Henssge, Rectal temperature time of death nomogram: Sudden change of ambient temperature. *Forensic Sci. Int.* **99**, 171–178 (1999).

20. E. A. den Hartog, W. A. Lotens, Postmortem time estimation using body temperature and a finite-element computer model. *Eur. J. Appl. Physiol.* **92**, 734–737 (2004).

21. G. Mall, W. Eisenmenger, Estimation of time since death by heat-flow Finite-Element model part II: Application to non-standard cooling conditions and preliminary results in practical casework. *Leg. Med.* **7**, 69–80 (2005).

22. S. Schenkl, H. Muggenthaler, M. Hubig, B. Erdmann, M. Weiser, S. Zachow, A. Heinrich, F. V. Güttler, U. Teichgräber, G. Mall, Automatic CT-based finite element model generation for temperature-based death time estimation: Feasibility study and sensitivity analysis. *Int. J. Leg. Med.* **131**, 699–712 (2017).

23. M. Weiser, B. Erdmann, S. Schenkl, H. Muggenthaler, M. Hubig, G. Mall, S. Zachow, Uncertainty in temperature-based determination of time of death. *Heat Mass Transf.* **54**, 2815–2826 (2018).

24. M. Weiser, Y. Freytag, B. Erdmann, M. Hubig, G. Mall, Optimal design of experiments for estimating the time of death in forensic medicine. *Inverse Probl.* **34**, 125005 (2018).

25. A. Luikov, *Analytical Heat Diffusion Theory* (Academic Press, 1968).

26. H. Muggenthaler, M. Hubig, S. Schenkl, G. Mall, Influence of hypo- and hyperthermia on death time estimation – A simulation study. *Leg. Med.* **28**, 10–14 (2017).

27. G. J. Edelman, M. C. Aalders, Photogrammetry using visible, infrared, hyperspectral and thermal imaging of crime scenes. *Forensic Sci. Int.* **292**, 181–189 (2018).

28. M. Hubig, S. Schenkl, H. Muggenthaler, F. Güttler, A. Heinrich, U. Teichgräber, G. Mall, Fully automatic CT-histogram-based fat estimation in dead bodies. *Int. J. Leg. Med.* **132**, 563–577 (2018).

29. Institute of Medicine, Food and Nutrition Board, Committee on Military Nutrition Research, Subcommittee on Military Weight Management, *Weight Management: State of the Science and Opportunities for Military Programs* (The National Academies Press, 2003).

30. I. P. Herman, *Physics of the Human Body* (Springer International Publishing, 2016), Biological and medical physics, biomedical engineering.

31. J.-J. Wu, H. Tang, Y.-X. Wu, A predictive model of thermal conductivity of plain woven fabrics. *Therm. Sci.* **21**, 1627–1632 (2017).

32. J. Steketee, Spectral emissivity of skin and pericardium. *Phys. Med. Biol.* **18**, 307 (1973).

33. G. Nellis, S. A. Klein, *Heat Transfer* (Cambridge Univ. Press, 2008).

34. K. Giering, I. Lamprecht, O. Minet, Specific heat capacities of human and animal tissues. *Proc. SPIE Int. Soc. Opt. Eng.* **2624**, 188–197 (1996).

35. S. Lee, C. Park, D. Kulkarni, S. Tamanna, T. Knox, Heat Transfer Division, in *2010 14th International Heat Transfer Conference*, (Washington DC, American Society of Mechanical Engineers, New York City, New York, 8 to 13 August 2010), pp. 619-628.

36. Y. Jhanji, D. Gupta, V. K. Kothari, Thermo-physiological properties of polyester–cotton plated fabrics in relation to fibre linear density and yarn type. *Fash. Text.* **2**, 16 (2015).

37. D. V. Schroeder, *An Introduction to Thermal Physics* (Addison Wesley, 1999).

38. A. T. Johnson, *Biological Process Engineering: An Analogical Approach to Fluid Flow, Heat Transfer, and Mass Transfer Applied to Biological System*s (Wiley, 1999).

39. B. Gebhart, L. Pera, The nature of vertical natural convection flows resulting from the combined buoyancy effects of thermal and mass diffusion. *Int. J. Heat Mass Transf.* **14**, 2025–2050 (1971).

40. J. van Kan, A. Segal, G. Segal, F. Vermolen, *Numerical Methods in Scientific Computing* (VSSD, 2005).